BIOCHEMISTRY
including biophysical chemistry & molecular biology

Article

pubs.acs.org/biochemistry

A Conserved Interdomain Interaction Is a Determinant of Folding Cooperativity in the GST Fold

Nishal Parbhoo,[†,§] Stoyan H. Stoychev,[†,§] Sylvia Fanucchi,[†] Ikechukwu Achilonu,[†] Roslin J. Adamson,[†] Manuel Fernandes,[‡] Samantha Gildenhuys,[†] and Heini W. Dirr*[,†]

[†]Protein Structure−Function Research Unit, School of Molecular and Cell Biology, University of the Witwatersrand, Johannesburg 2050, South Africa

[‡]School of Chemistry, University of the Witwatersrand, Johannesburg 2050, South Africa

Supporting Information

ABSTRACT: The canonical glutathione transferase (GST) fold found in many monomeric and dimeric proteins consists of two domains that differ in structure and conformational dynamics. However, no evidence exists that the two domains unfold/fold independently at equilibrium, indicating the significance of interdomain interactions in governing cooperativity between domains. Bioinformatics analyses indicate the interdomain interface of the GST fold is large, predominantly hydrophobic with a high packing density explaining cooperative interdomain behavior. Structural alignments reveal a topologically conserved lock-and-key interaction across the domain interface in which a bulky hydrophobic residue ("key") protrudes from the surface of the N-domain and inserts into a pocket ("lock") in the C-domain. To better understand the molecular basis for the contribution of interdomain interactions toward cooperativity within the GST fold in the absence of any influence from quaternary interactions, studies were done with two monomeric GST proteins: *Escherichia coli* Grx2 (EcGrx2) and human CLIC1 (hCLIC1). Replacing the methionine "key" residue with alanine is structurally nondisruptive, whereas it significantly diminishes the folding cooperativity of both proteins. The loss in cooperativity between domains in the mutants is reflected by a change in the equilibrium folding mechanism from a wild-type two-state process to a three-state process, populating a stable folding intermediate.

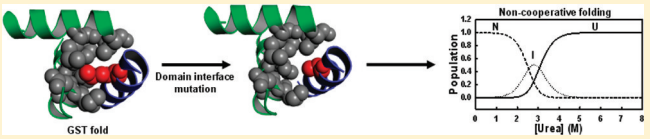

The structures of most pro- and eukaryotic proteins are composed of multiple domains.[1] While domains are traditionally thought of as autonomous folding units, interactions between domains can contribute significantly toward the structure and function of multidomain proteins.[2−4] It is therefore of interest to understand how interdomain interactions contribute toward the stability and cooperative behavior between domains in multidomain proteins.

Cytosolic glutathione transferases (GSTs) are a large family of multifunctional monomeric and dimeric proteins that have a canonical GST fold composed of two structurally distinct domains: an N-domain with a thioredoxin-like fold and a larger all-helical C-domain[5] (for example, see Figure 1). The GST fold is proposed to have evolved from a thioredoxin/glutaredoxin progenitor to which a unique C-terminal domain was added.[6] The diverse functionality of the GST family is reflected by its participation in a variety of catalytic and noncatalytic processes such as phase II detoxification and redox reactions, intracellular binding and transport of ligands, regulation of signaling pathways, and the formation of ion channels (reviewed in refs 7 and 8). The stability and dynamic nature of the domain interface influence catalysis and functional selectivity at the active site,[9−11] which is located along the domain interface having a G-site for glutathione on the N-domain and an adjacent H-site for hydrophobic substrates on both N- and C-domains. The domain interface is also implicated in the structural rearrangements required for the N-domain of soluble CLIC proteins to become membrane bound.[12]

Despite the structural and stability differences displayed by the domains,[13−15] the two domains in the native structure of the wild-type GST fold behave as a single cooperative folding unit under equilibrium conditions at pH 6.5−7.[16−22] Interdomain interactions, therefore, stabilize the domains and confer interdomain cooperativity.[9,14,23] Most studies on the stability and folding of GSTs have focused on the dimeric forms, thus complicating efforts to establish the role of interdomain interactions alone since certain quaternary interactions also form interdomain contacts.[23] However, it was demonstrated recently that in the absence of quaternary interactions the two domains in the GST fold of monomeric EcGrx2 and hCLIC1 can behave as a single cooperative folding unit at equilibrium.[12,24]

Here we investigate the molecular basis for cooperativity between domains of the GST fold without any influence from quaternary interactions. Bioinformatics analyses indicate the interdomain interface of the GST fold to be large and predominantly hydrophobic with a high packing density. Structural alignments revealed a topologically conserved lock-and-key

Received: April 28, 2011
Revised: June 17, 2011
Published: July 7, 2011

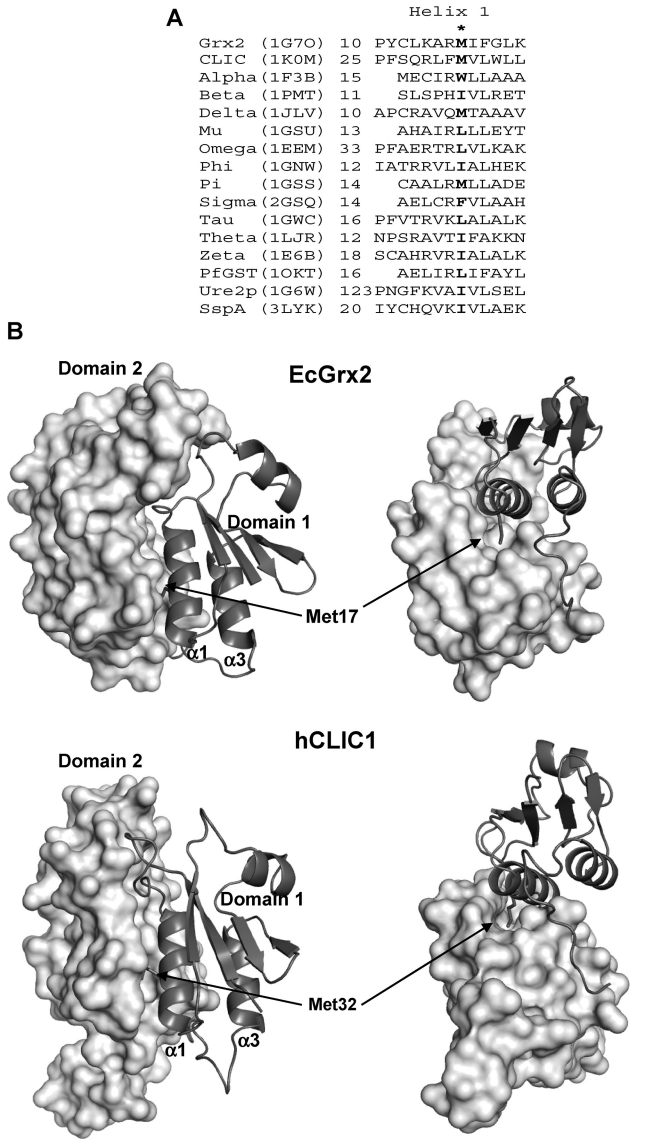

Figure 1. Interdomain "lock-and-key" motif in GST fold. (A) Structurally aligned sequences of helix 1, indicating the topologically conserved key residue (asterisk) in the representative GST structures. PDB codes in parentheses. (B) Structures of wild-type EcGrx2 (PDB code 1G7O) and hCLIC1 (PDB code 1K0M) depicting domain 1 in ribbon format and domain 2 in molecular surface format. The conserved key residue in helix 1 (Met17 in EcGrx2 and Met32 in hCLIC1) are shown as sticks. The structures were aligned with UCSF Chimera,[38] and the images were generated with PyMOL (DeLano Scientific, San Carlos, CA).

interaction across the domain interface in which a bulky hydrophobic residue ("key") protrudes from the surface of the N-domain and inserts into a pocket ("lock") in the C-domain. Replacing the key residue in EcGrx2 and hCLIC1 with an alanine is structurally nondisruptive, whereas the folding cooperativity of both monomeric proteins are diminished resulting in the accumulation of an intermediate.

EXPERIMENTAL PROCEDURES

Materials. 8-Anilino-1-naphthalenesulfonic acid (ANS) was purchased from Sigma-Aldrich (St. Louis, MO). DTT and IPTG were purchased from Fermentas Life Sciences (St. Leon-Rot, Germany). DEAE-Sepharose and Sephadex G-75 were purchased from GE Healthcare Life Sciences (Uppsala, Sweden). Ultrapure (99.5%) urea was purchased from Merck chemicals (Darmstadt, Germany). All other reagents were of analytical grade.

Mutagenesis, Protein Overexpression, and Purification. Met-to-Ala mutants were generated by site-directed mutagenesis (Stratagene QuickChange II, La Jolla, CA) using recombinant plasmids that code for wild-type EcGrx2 (a gift from from J. Dyson, The Scripps Institute, La Jolla, CA) and wild-type hCLIC1 (a gift from S. Breit, St Vincent's Hospital and University of New South Wales, Australia). The primers used for generating the M17A EcGrx2 mutant were:

forward: 5′CTTACTGTCTCAAAG*CT*CGCGCAATTTTCGGCCTG*AAG*AATATC3′

reverse: 5′GATATT*CTT*CAGGCCGAAAATTGCGC*GAGC*TTTGAGACAGTAAG3′

Those for the M32A hCLIC1 mutant were:

forward: 5′CATTCTCCCAGAGACTGTTCGCGGTACTGTGGCTCAAGGGAG3′

reverse: 5′CTCCCTTGAGCCACAGTACCGCGAACAGTCTCTGGGAGAATG3′

The underlined bases represent the Met-to-Ala mutations, and those in italics are silent mutations to avoid hairpin and loop formation. These mutations and the absence of other mutations were confirmed by DNA sequencing (Inqaba Biotech, Pretoria, South Africa).

Wild-type and M32A hCLIC1 and wild-type EcGrx2 were overexpressed in *Escherichia coli* BL21(DE3)pLysS,[25] and M17A EcGrx2 was overexpressed in T7 Express I^q competent cells (New England Biolabs Inc., Ipswich, MA). The proteins were purified as previously described[12,24,25] and stored in 50 mM sodium phosphate buffer, pH 7.0, 1 mM DTT, and 0.02% (w/v) NaN_3. Protein purity and size were assessed by SDS-PAGE and SE-HPLC.

Spectroscopy. Far- and near-UV CD spectra of EcGrx2 and hCLIC1 in 5 mM sodium phosphate buffer, pH 7.0, 1 mM DTT, and 0.02% (w/v) NaN_3 were recorded with a Jasco J-810 spectropolarimeter at 20 and 5 °C, respectively, and represent an average of 10 accumulations. Fluorescence measurements (average of three accumulations) were made at 20 °C using a Perkin-Elmer luminescence spectrometer LS50B. All spectra were corrected for buffer.

Urea-Induced Equilibrium Unfolding. Protein (2 μM) was incubated with 0 to 8 M urea in 50 mM sodium phosphate buffer, pH 7.0, 1 mM DTT, and 0.02% (w/v) NaN_3, at 20 °C followed by far-UV CD, tryptophan fluorescence (excitation at 295 nm), ANS binding, and light scattering measurements.[12,24] ANS binding was performed by adding 200 μM ANS (final concentration) to protein in 0−8 M urea and measuring ANS fluorescence (excitation at 390 nm). Light scattering (excitation and emission wavelengths at 340 nm) was performed to monitor protein aggregation.

Fluorescence and CD unfolding data were globally fit,[26] using the linear extrapolation method,[27] to either a two-state monomer (N ↔ U) or a three-state monomer (N ↔ I ↔ U) model using Savuka version 6.2.26.[28,29] The thermodynamic parameters, $\Delta G(H_2O)$ and *m*-value, obtained from the global fits were used to calculate the fractional populations of each species from the equilibrium constants.

Crystallization and Structure Determination. For crystallization trials, M32A hCLIC1 was passed through a

Sephadex G-75 size-exclusion column (Amersham Biosciences) equilibrated with 0.1 M Tris-HCl, 1 mM DTT and 0.02% sodium azide, pH 6.5. Crystals of M32A hCLIC1 were grown by the hanging drop vapor diffusion method at 293 K using 24-well microplates. Each hanging drop (4, 6, and 8 μL) comprised of an equal volume of stock protein solution (10 mg/mL) and reservoir buffer (20% w/v PEG 3350 in 0.1 M Tris-HCl, 0.2 M NaCl, 1 mM DTT, and 0.02% NaN_3, pH 6.5). The crystals were harvested, briefly soaked in the reservoir buffer and mounted on a cryoloop.

Diffraction data were collected at 113 K using a Bruker X8 Proteum system with a copper rotating anode generator with Montel 200 optics, a Platinum 135 CCD detector, and an Oxford Cryostream Plus system. The data were processed using SAINT and APEX software (Bruker AXS Inc., Madison, WI). The phases were determined by molecular replacement with Phaser[30] in the CCP4i suite of programmes[31] using wild-type hCLIC1 (PDB code: 1K0M[32]) as the search model. The structure was modeled using TLS refinement as implemented in REFMAC5.[33] This was followed by coordinate and B-factor refinement in REFMAC5. Model building, addition of water molecules, and preliminary validation were performed using Coot.[34] The final model was validated using both PROCHECK[35] and MolProbity.[36]

***In Silico* Analysis of the Domain Interface of GSTs.** The superfamily of cytosolic GSTs has been classified into a number of family-like classes (http://scop.mrc-lmb.cam.ac.uk/scop/index.html[37]). Our data set used for analyzing the physicochemical properties of the domain interface of GSTs consisted of a structural representative from each of the major GST classes (excluding kappa GST which does not have a canonical GST fold) and other "unclassified" GST-like proteins: alpha (1F3B), beta (1PMT), delta (1JLV), mu (1GSU), omega (1EEM), phi (1GNW), pi (1GSS), sigma (2GSQ), tau (1GWC), theta (1LJR), zeta (1E6B), *Plasmodium falciparum* GST (1OKT), yeast Ure2p (1G6W), *Haemophilus influenzae* stringent starvation protein A (3LYK), *Escherichia coli* EcGrx2 (1G7O), and hCLIC1 (1K0M). The sequence identity of the representative set of structures ranges from 6 to 28% as determined by structure-based sequence alignment using UCSF Chimera.[38]

Each GST monomer consists of two structurally distinct domains and the PROTORP server (http://www.bioinformatics.sussex.ac.uk/protorp/[39]) was used to determine physicochemical parameters for the interfaces between these domains. Each PDB file submitted to the server was first edited to include only one subunit/monomer and to exclude the linker region connecting the two domains so that each file consisted of two chains: chain N for the N-domain and chain C for the C-domain. The sequence corresponding to each domain in the structural data set is given in Supporting Information Table S1.

RESULTS

Analysis of the Domain Interface of Proteins with a GST Fold. The values of the physicochemical parameters for the domain interfaces in EcGrx2 and hCLIC1 as well as the average values for our structural data set are presented in Table 1. The details for all 16 representatives in our data set are shown in Table S1 of the Supporting Information. These features are characteristic for interfaces of permanent protein−protein interactions,[40,41] suggesting the existence of strong interactions across the domain interface that would maintain a global structural communication within the GST fold. The scaffold of the interface between the two domains in the GST fold is predominantly α-helical with helix 1 from the N-domain as a major source of interdomain interactions. A topologically conserved interdomain lock-and-key motif was identified by inspection of the aligned GST structures in which the side chain of a hydrophobic residue (the "key") in helix 1 (marked with an asterisk in Figure 1A) extends across the domain interface and interacts with a pocket (the "lock") in the C-domain, as shown in Figure 1B for EcGrx2 and hCLIC1. This structurally conserved and solvent-inaccessible motif at the domain interface could function as a hot spot[42] that contributes cooperatively toward the stability of the GST fold.

Table 1. Physicochemical Features of the Domain Interface in GST Proteins[a]

		average (range)[b]	EcGrx2	hCLIC1
interface ΔASA/domain (Å^2)	N[c]	996.7 (760−1366)	1018	914
	C[c]	946.1 (679−1228)	970	872
total interface ΔASA (Å^2)		1942.8 (1446−2593)	1988	1786
% interface ΔASA/domain	N	19.6 (15.3−24.4)	23	16
	C	12.1 (9.2−15.3)	13	11
no. of residues in interface	N	21 (17−30)	21	19
	C	26.6 (19−33)	29	25
% polar residues at interface	N	24 (5−38)	19	26
	C	27 (7−40)	31	32
% nonpolar residues at interface	N	50 (29−75)	57	47
	C	51 (32−67)	48	44
planarity (Å)		2.83 (2.10−4.23)	2.97	2.10
gap volume (Å^3)		3948 (3189−5373)	3200	3189
gap volume index (Å)		2.08 (1.51−3.38)	1.61	1.79
H-bonds		6.6 (3−10)	4	4

[a]The PROTORP server (http://www.bioinformatics.sussex.ac.uk/protorp/[39]) was used to determine physicochemical parameters for the interfaces between the N- and C-domains. The interface parameters are defined at http://www.bioinformatics.sussex.ac.uk/protorp/params.html. [b]Average values for the data set of 16 structures. The range of the individual values in the data set are given in parentheses. [c]N and C refer to the N- and C-domains, respectively.

Structural Characterization of the EcGrx2 and hCLIC1 Mutants. To investigate the role of a conserved interdomain motif in the structure and stability of the GST fold without any influence from quaternary interactions, the key residue in monomeric EcGrx2 and hCLIC1 (Met17 and Met32, respectively) were mutated to an alanine. Crystallization experiments were successful only for M32A hCLIC1, and its structure was solved and refined to a resolution of 1.7 Å by molecular replacement (Table 2). The electron density of the final model is well-defined for residues 6−241 with the electron density for residue 32 being consistent with that for an alanine residue. The M32A mutation does not alter the backbone structure, as indicated by the Cα rmsd value of 0.56 Å between the wild-type (PDB code 1K0M) and M32A hCLIC1 structures. Moreover, the cavity creating M32A mutation does not change the local structure at the domain interface (Figure 2).

For M17A EcGrx2, spectroscopic methods were used to establish the integrity of the protein's structure. The CD and

Table 2. X-ray Diffraction Data Collection and Refinement Statistics for M32A hCLIC1

wavelength (Å)	1.5418
space group	$P2_12_12_1$
unit-cell parameter *a*, *b*, *c* (Å)	42.36, 63.99, 82.80
Wilson plot *B*-factor (Å^2)	13.3
resolution range (Å)	50.63−1.69 (1.75−1.69)[a]
no. of observed reflections	274 792
no. of unique reflections	25 463
completeness	98.6
$\langle I/\sigma(I)\rangle$	24.5 (3.87)
R_{sym}[b]	0.156 (0.641)
final overall *R* factor	0.211
R_{work}	0.231 (0.334)
R_{free}	0.271 (0.401)
no. of protein atoms	1851
no. of ligand atoms	0
total no. of atoms	2001
Matthew's coefficient V_M (Å^3 Da^{1-})	2.13
solvent content (%)	42.34
average *B*-value (Å^2)	17.45
rmsd bond length (Å)	0.025
rmsd bond angles (deg)	2.028
Ramachandran statistics most favored (%)	93.8
allowed (%)	5.8
generously allowed (%)	0.4
asymmetric unit content	monomer
PDB code	3O3T

[a]The values in parentheses are for the highest resolution shell. [b]$R_{sym} = \sum_{hkl}\sum_i|I_i(hkl) - \langle I(hkl)\rangle|/\sum_{hkl}\sum_i I_i(hkl)$, where $I(hkl)$ is the intensities of reflection *hkl*, $\sum_{hkl}$ is the sum overall of all reflections, and $\sum_i$ is the sum over *i* measurements of reflection *hkl*, R_{free} is calculated for a randomly chosen 5% of reflections which were not used for refinement of structure, and R_{work} is calculated for the remaining reflections.

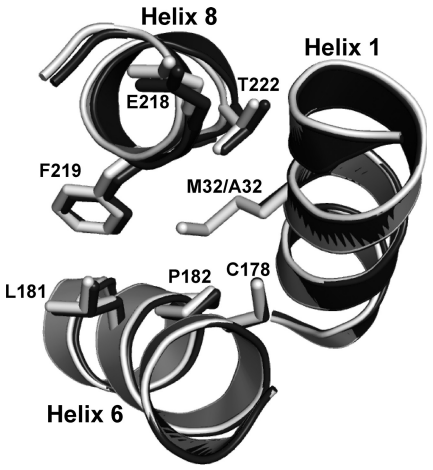

Figure 2. Structural elements of the interdomain lock-and-key motif in hCLIC1. Structural features at the domain interface of wild-type (light gray; PDB code 1K0M) and M32A (dark gray; PDB code 3O3T) hCLIC1 showing the interdomain lock-and-key motif. Image was generated with PyMOL (DeLano Scientific, San Carlos, CA).

fluorescence spectral data shown in Figure 3 are essentially the same for both wild-type and M17A EcGrx2, indicating that the mutation is not disruptive.

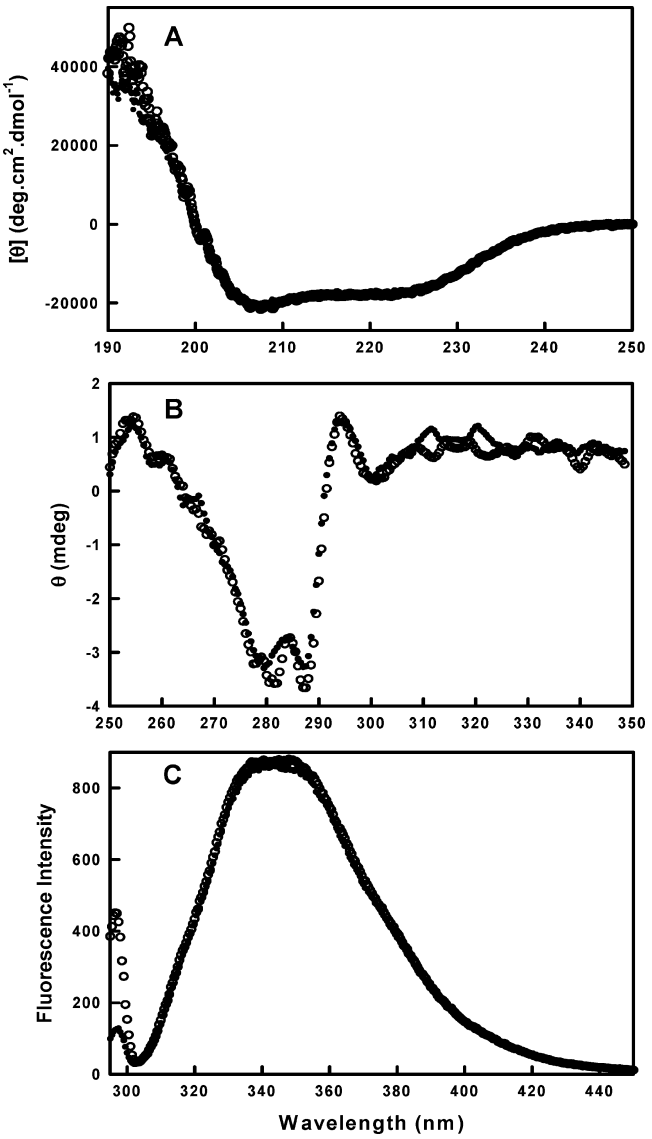

Figure 3. Structural characterization of EcGrx2. Spectra representing the secondary and tertiary structural characteristics of wild-type (●) and M17A (○) EcGrx2 in 5 mM sodium phosphate buffer, pH 7.0, 1 mM DTT, and 0.02% (w/v) NaN_3. (A) Far-UV CD spectra of 5 μM protein at 20 °C. (B) Near-UV CD spectra of 40 μM protein at 5 °C. (C) Tryptophan fluorescence emission spectra of 5 μM protein excited at 295 nm (20 °C).

Conformational Stability of M17A EcGrx2 and M32A hCLIC1. Equilibrium urea denaturation studies were performed to determine the conformational stability of the two Met-to-Ala mutants. A thermodynamic explanation of the structural transitions obtained from these experiments requires that the unfolding and refolding processes be reversible. Chemical denaturation with urea, as monitored by far-UV CD at 222 nm and tryptophan fluorescence, was shown to be reversible for the wild-type proteins[12,24] and, in this study, by the recovery of >95% of the far-UV CD and fluorescence signals after the denatured mutants in 8 M urea were refolded in 0.8 M urea by a 10-fold dilution with buffer.

The equilibrium folding transitions for M32A hCLIC1 (Figure 4A, top panel) do not display the two-state behavior observed for the wild-type protein at pH 7.[12] The biphasic

dx.doi.org/10.1021/bi2006509|*Biochemistry* 2011, 50, 7067−7075

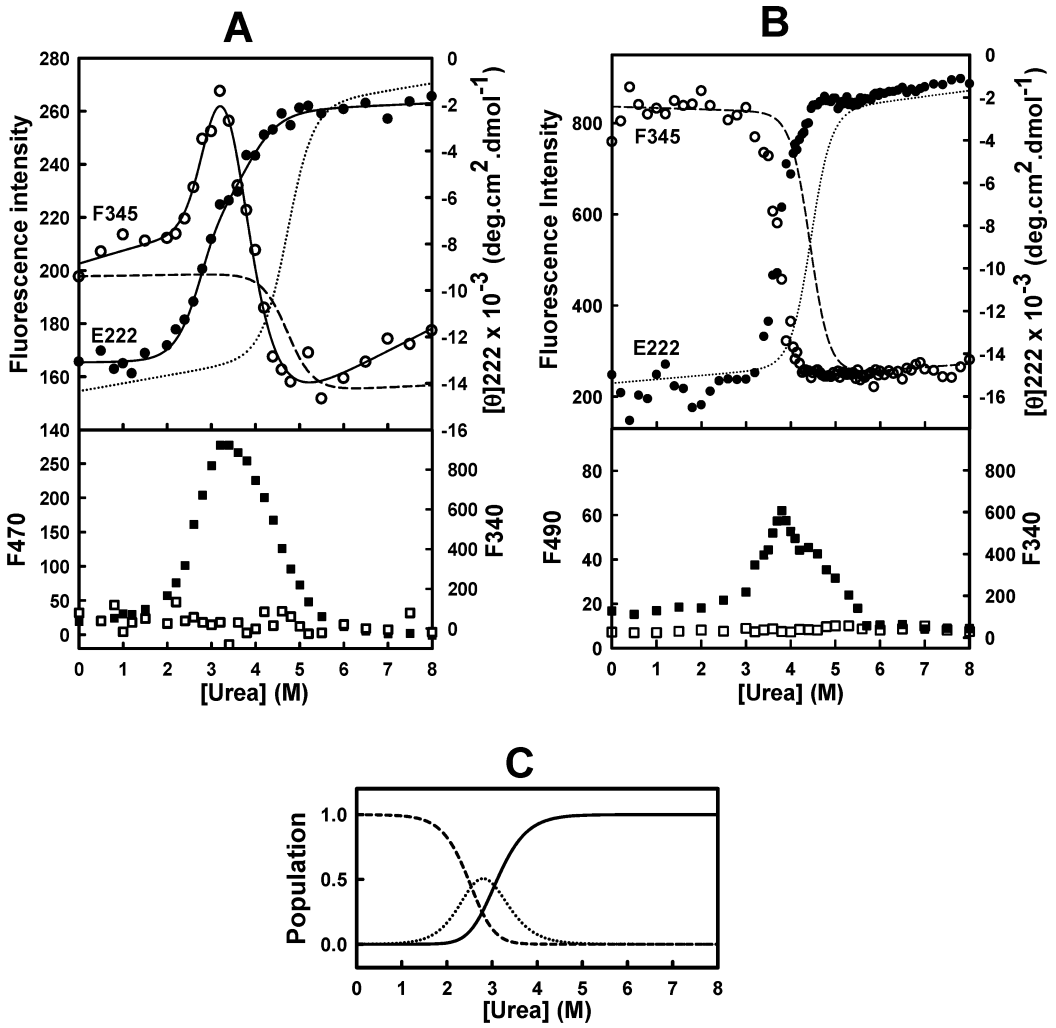

Figure 4. Equilibrium unfolding of M32A hCLIC1 and M17A EcGrx2. Protein concentration was 2 μM in 50 mM sodium phosphate, pH 7.0, 1 mM DTT, and 0.02% (w/v) NaN_3. (A) M32A hCLIC1 and (B) M17A EcGrx2 unfolding curves monitored by spectroscopy (upper panels) and by ANS binding (lower panels). (○) Fluorescence intensity at 345 nm (excitation of 295 nm), (●) CD ellipticity at 222 nm, (■) ANS fluorescence in the presence of mutant protein, (□) light scattering signal with excitation and emission wavelengths set at 340 nm. The three-state fits by nonlinear regression for M32A hCLIC1 in (A) are in solid lines. The two-state global fits to the data for wild-type hCLIC1[12] and EcGrx2[24] are shown for comparison: fluorescence at 345 nm (···) and CD ellipticity at 222 nm (- - -); $\Delta G(H_2O)$ = 8.0 ± 0.5 kcal mol^{-1} and m value =1.7 ± 0.11 kcal mol^{-1} (M urea)$^{-1}$ for wild-type hCLIC1, and $\Delta G(H_2O)$ = 12.92 ± 0.77 kcal mol^{-1} and m value =2.9 ± 0.17 kcal mol^{-1} (M urea)$^{-1}$ for wild-type EcGrx2. (C) Fractional populations of the native (- - -), intermediate (···), and unfolded (—) states as a function of urea concentration for M32A hCLIC1. The populations were calculated using the thermodynamic parameters obtained from globally fitting the data to a three-state model (see Table 3).

transitions for both fluorescence and CD indicate that the mutation results in the formation of a stable intermediate between 2 and 3.2 M urea followed by its unfolding at higher urea concentrations. Formation of the intermediate results in an increase in fluorescence intensity accompanied by a blue shift from 345 to 340 nm in the maximum emission wavelength of Trp35 (data not shown) and a loss of about 50% in the ellipticity at 222 nm (Figure 4A, upper panel). This intermediate also binds the amphipathic dye ANS displaying maximal binding at 3.2 M urea (Figure 4A, bottom panel). The hydrophobic nature of the surface to which ANS binds is confirmed by the blue shift from 530 to 470 nm in the emission maximum of ANS when the dye binds to the intermediate at 3.2 M urea (Figure 5A). The ability of tryptophan fluorescence to reveal the formation of the intermediate is because the only tryptophan in hCLIC1 (Trp35) is located close to Met32 in helix 1 at the domain interface and, therefore, serves as a local probe. The data for M32A hCLIC1 fitted well to a three-state (N ↔ I ↔ U) model, and the parameters are shown in Table 3. The calculated population distribution of native, intermediate, and unfolded states for M32A hCLIC1 using the values from the three-state fit is shown in Figure 4C, indicating that the concentration of the intermediate peaks at 3.2 M urea.

The equilibrium denaturation transitions for M17A EcGrx2 shown in the top panel of Figure 4B appear to be monophasic for the spectroscopic changes (fluorescence and ellipticity) suggesting a two-state process, as reported for the wild-type.[24] The transitions for the M17A mutant are, however, shifted to lower urea concentrations (C_m = 3.7 M) when compared to those of the wild-type (C_m = 4.8 M). Further, and unlike the wild-type protein which has been shown not to bind ANS at any point along its unfolding transition,[24] the M17A mutant binds ANS between 3 and 5.5 M urea with maximal binding

dx.doi.org/10.1021/bi2006509 | Biochemistry 2011, 50, 7067–7075

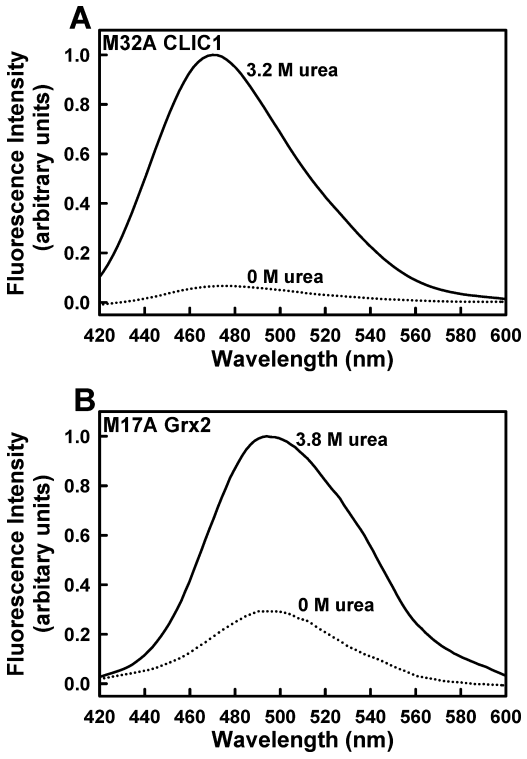

Figure 5. Emission spectra of protein-bound ANS. Protein and ANS concentrations were 2 and 200 μM, respectively, in 50 mM sodium phosphate buffer, pH 7.0, 1 mM DTT, and 0.02% (w/v) NaN_3 in the absence or presence of urea as indicated. (A) M32A hCLIC1 and (B) M17A EcGrx2. Excitation was at 390 nm.

occurring at 3.8 M urea (Figure 4B, bottom panel), thus revealing the existence of an intermediate state with solvent-exposed hydrophobic patches. The latter is demonstrated by the observed blue-shift from 530 to 490 nm in the emission maximum wavelength of ANS when the dye binds to the intermediate (Figure 5A). The presence of a populated intermediate indicates that the unfolding is not two-state as suggested by the spectroscopic data. Although these data do fit well to a two-state model (not shown), application of this assumption can result in a large underestimation of the free energy of unfolding.[43,44] However, attempts to fit the data to a three-state model were not satisfactory. Although the residuals for the three-state fit appeared to indicate a "good" fit, the errors for the thermodynamic parameters were very large. Because the C-domain contains 79% of the protein's secondary structure as well as both tryptophan residues (Trp89 and Trp190 which are about 20 Å from Met17), it is possible that the spectroscopic probes used to monitor equilibrium folding were insensitive to the formation of the M17A intermediate, thus explaining the apparent two-state behavior.

Light scattering data for both M17A EcGrx2 (Figure 4A, bottom panel) and M32A hCLIC1 (Figure 4B, bottom panel) excluded the presence of protein aggregation during unfolding.

DISCUSSION

Proteins with a GST fold exist either as stable monomers or as stable dimers. While HXMS data reveal the N-domain to be conformationally more dynamic than the larger C-domain in the GST fold,[14,15] equilibrium denaturation studies demonstrate that the two domains fold cooperatively.[16−22] The analysis of the physicochemical properties of the domain interface in GST proteins reported here indicates the interface to be large and predominantly hydrophobic with a high packing density (Table 1 and Table S1) explaining the cooperative behavior.[3] However, the molecular basis (i.e., specific interactions involved) for this interdomain cooperativity is unknown. While cooperativity between domains in the GST fold was proposed to be maintained primarily by interactions between the C-domain and helix 3 in the N-domain,[13,45−47] crystallographic data indicate that helix 1 rather than helix 3 is the major source of interdomain contacts with the neighboring C-domain. Furthermore, data from recent amide HXMS experiments disclose a cooperative link, via helix 1, between the N- and C-domains.[14,15] An alignment of GST structures indicates that helix 1 contains a buried hydrophobic "key" residue in a topologically conserved lock-and-key interdomain motif that protrudes from the surface of the N-domain and inserts into a pocket ("lock") in the C-domain (Figure 1). Protruding residues that are inaccessible to solvent are one of the most important geometric features of hot spots at protein interfaces that contribute significantly toward binding free energy.[48,49] While the lock-and-key motif referred to above occurs between the two domains within the same monomer, some classes of dimeric GSTs (alpha, mu, pi) display a hydrophobic lock-and-key motif across their dimer interface that forms stabilizing interactions between the N-domain of one subunit and the C-domain of the other subunit.[14,50−55]

Since certain intersubunit interactions in dimeric GSTs are also involved in interdomain contacts,[23] the contribution of the conserved interdomain lock-and-key motif toward the stability and interdomain cooperativity was investigated with two monomeric representatives of the GST fold (EcGrx2 and hCLIC1) in order to preclude any influence from quaternary interactions. The two-domain structure of wild-type EcGrx2 and hCLIC1 unfolds as single cooperative unit in a two-state equilibrium manner at pH 6.5−7 and 20 °C with only the folded native state and the denatured state being populated (N ↔ U).[12,24] Disruption of the interdomain lock-and-key interaction by replacing the "key" methionine residue with an alanine, however, is shown in this study to alter the equilibrium folding mechanism of the GST fold to a three-state (N ↔ I ↔ U) process in which an intermediate state becomes significantly populated. While the amino acid substitution does not alter the native structures of EcGrx2 and hCLIC1, the accumulation of an intermediate signifies a loss in cooperativity within their structures. Three-state folding behavior was more clearly evident for M32A hCLIC1 which produced biphasic CD and fluorescence transitions whereas M17A EcGrx2 displays monophasic and apparently cooperative transitions (Figure 4). Nevertheless, formation of a stable, partially folded intermediate

Table 3. Equilibrium Thermodynamic Stability Parameters for hCLIC1

three-state fit	$\Delta G(H_2O)_{N-I}$ (kcal mol^{-1})	m_{N-I} (kcal mol^{-1} M^{-1})	$\Delta G(H_2O)_{I-U}$ (kcal mol^{-1})	m_{I-U} (kcal mol^{-1} M^{-1})
M32A hCLIC1	5.3 ± 0.86	1.8 ± 0.39	5.53 ± 1.54	1.6 ± 0.31

[a]Parameters were obtained by global fitting of fluorescence and CD equilibrium urea denaturation curves using SAVUKA.[28,29]

dx.doi.org/10.1021/bi2006509 | Biochemistry 2011, 50, 7067−7075

by both mutant proteins was demonstrated by the binding of ANS, a probe used widely to detect and characterize intermediate states. The fluorescence properties of ANS indicate that the dye-binding regions exposed during the formation of the EcGrx2 intermediate state are not as hydrophobic as those exposed in the hCLIC1 intermediate.

Though wild-type hCLIC1 does not form an unfolding intermediate at pH 7, it displays three-state folding behavior (N ↔ I ↔ U) at pH 5.5 which is proposed to be involved in priming the soluble form of the protein for its insertion into membranes.[12] Spectroscopic and ANS binding data (this study and in ref 12) indicate that the features of the M32A intermediate formed at pH 7 appear to be similar to those of the wild-type intermediate formed at pH 5.5. Both display ~50% of the native structure, a burial of Trp35 in a more hydrophobic environment, and ANS binding to a hydrophobic surface. While the basis for the pH-dependent formation of the wild-type hCLIC1 intermediate is unknown, Met32-mediated interdomain cooperativity appears to play a role.

The extent to which cooperativity is lost between the domains as a consequence of the mutation at the domain interface appears to be less for EcGrx2 than that for hCLIC1. The domain interface in EcGrx2 buries about 200 Å^2 more accessible surface area than that for hCLIC1 (Table 1), accounting for more stabilizing contacts and a tighter coupling between the EcGrx2 domains. Although the conserved lock-and-key motif at the domain interface of the GST fold is an important determinant of interdomain cooperativity, its disruption does not cause each domain to unfold independently of the other. Should they unfold independently, the smaller and more dynamic N-domain (which contains about 20% of the total secondary structure) would be expected to unfold at urea concentrations lower than those for the larger C-terminal domain. However, although two CD transitions are observed for M32A hCLIC1, the first transition at lower urea concentrations (i.e., intermediate formation) reports a loss of about 50% of the CD signal which is far greater than that expected for the unfolding of only the N-domain. Furthermore, the changes observed in the fluorescence signal are not consistent with independent domain unfolding. hCLIC1 has one tryptophan in its N-domain and none in the C-domain while both tryptophans in EcGrx2 are located in its C-domain. However, the fluorescence unfolding curves do not display an N-domain-only transition for hCLIC1 or a C-domain-only transition for EcGrx2.

■ ASSOCIATED CONTENT

Ⓢ Supporting Information

Domain interface parameters for GST proteins (Table S1). This material is available free of charge via the Internet at http://pubs.acs.org.

■ AUTHOR INFORMATION

Corresponding Author

*Phone: +27 11 7176352. Fax: +27 11 7176351. E-mail: heinrich.dirr@wits.ac.za.

Author Contributions

§These authors contributed equally to this work.

Funding

This work was supported by the University of the Witwatersrand, South African National Research Foundation (grants 60810, 65510, and 68898 to H.W.D.), and South African Research Chairs Initiative of the Department of Science and Technology and National Research Foundation (grant 64788 to H.W.D.).

■ ABBREVIATIONS

CD, circular dichroism; DEAE, diethylaminoethyl; DTT, dithiothreitol; EcGrx2, glutaredoxin 2 from *Escherichia coli*; GST, glutathione transferase; hCLIC1, chloride intracellular channel protein 1 from human; SASA, solvent accessible surface area; SCOP, Structural Classification of Proteins; SE-HPLC, size exclusion high-performance liquid chromatography; IPTG, isopropyl β-D-1-thiogalactopyranoside; ANS, 8-anilino-1-naphthalenesulfonic acid; HXMS, hydrogen exchange mass spectroscopy.

■ REFERENCES

(1) Teichmann, S. A., Chothia, C., and Gerstein, M. (1999) Advances in structural genomics. *Curr. Opin. Struct. Biol. 9*, 390−399.

(2) Jaenicke, R. (1999) Stability and folding of domain proteins. *Prog. Biophys. Mol. Biol. 71*, 155−241.

(3) Han, J. H., Batey, S., Nickson, A. A., Teichmann, S. A., and Clarke, J. (2007) The folding and evolution of multidomain proteins. *Nature Rev. 8*, 319−330.

(4) Batey, S., Nickson, A. A., and Clarke, J. (2008) Studying the folding of multidomain proteins. *HFSP J. 2*, 365−377.

(5) Dirr, H., Reinemer, P., and Huber, R. (1994) Refined crystal structure of porcine class Pi glutathione S-transferase (pGST P1−1) at 2.1 Å resolution. *Eur. J. Biochem. 220*, 645−661.

(6) Armstrong, R. N. (1997) Structure, catalytic mechanism, and evolution of the glutathione transferases. *Chem. Res. Toxicol. 10*, 2−18.

(7) Sheehan, D., Meade, G., Foley, V. M., and Dowd, C. A. (2001) Structure, function and evolution of glutathione transferases: implications for classification of non-mammalian members of an ancient enzyme superfamily. *Biochem. J. 360*, 1−16.

(8) Oakley, A. J. (2005) Glutathione transferases: new functions. *Curr. Opin. Struct. Biol. 15*, 716−723.

(9) Wallace, L. A., Burke, J., and Dirr, H. W. (2000) Domain-domain interface packing at conserved Trp-20 in class alpha glutathione transferase impacts on protein stability. *Biochim. Biophys. Acta 1478*, 325−332.

(10) Balchin, D., Fanucchi, S., Achilonu, I., Adamson, R. J., Burke, J., Fernandes, M., Gildenhuys, S., and Dirr, H. W. (2010) Stability of the domain interface contributes towards the catalytic function at the H-site of class alpha glutathione transferase A1−1. *Biochim. Biophys. Acta 1804*, 2228−2233.

(11) Hou, L., Honaker, M. T., Shireman, L. M., Balogh, L. M., Roberts, A. G., Ng, K. C., Nath, A., and Atkins, W. M. (2007) Functional promiscuity correlates with conformational heterogeneity in A-class glutathione S-transferases. *J. Biol. Chem. 282*, 23264−23274.

(12) Fanucchi, S., Adamson, R. J., and Dirr, H. W. (2008) Formation of an unfolding intermediate state of soluble chloride intracellular channel protein CLIC1 at acidic pH. *Biochemistry 47*, 11674−11681.

(13) Dragani, B., Iannarelli, V., Allocati, N., Masulli, M., Cicconetti, M., and Aceto, A. (1998) Irreversible thermal denaturation of glutathione transferase P1−1. Evidence for varying structural stability of different domains. *Int. J. Biochem. Cell Biol. 30*, 155−163.

(14) Thompson, L. C., Walters, J., Burke, J., Parsons, J. F., Armstrong, R. N., and Dirr, H. W. (2006) Double mutation at the subunit interface of glutathione transferase rGSTM1−1 results in a stable, folded monomer. *Biochemistry 45*, 2267−2273.

(15) Stoychev, S. H., Nathaniel, C., Fanucchi, S., Brock, M., Li, S., Asmus, K., Woods, V. L. Jr., and Dirr, H. W. (2009) Structural dynamics of soluble chloride intracellular channel protein CLIC1 examined by amide hydrogen-deuterium exchange mass spectrometry. *Biochemistry 48*, 8413−8421.

(16) Dirr, H. W., and Reinemer, P. (1991) Equilibrium unfolding of class pi glutathione S-transferase. *Biochem. Biophys. Res. Commun. 180*, 294−300.

(17) Erhardt, J., and Dirr, H. (1995) Native dimer stabilises the subunit tertiary structure of porcine class pi glutathione S-transferase. *Eur. J. Biochem. 230*, 614−620.

(18) Kaplan, W., Husler, P., Klump, H., Erhardt, J., Sluis-Cremer, N., and Dirr, H. (1997) Conformational stability of pGEX-expressed *Schistosoma japonicum* glutathione S-transferase: a detoxification enzyme and fusion-protein affinity tag. *Protein Sci. 6*, 399−406.

(19) Wallace, L. A., Sluis-Cremer, N., and Dirr, H. W. (1998) Equilibrium and kinetic unfolding properties of dimeric human glutathione transferase A1−1. *Biochemistry 37*, 5320−5328.

(20) Stevens, J. M., Hornby, J. A., Armstrong, R. N., and Dirr, H. W. (1998) Class sigma glutathione transferase unfolds via a dimeric and a monomeric intermediate: impact of subunit interface on conformational stability in the superfamily. *Biochemistry 37*, 15534−15541.

(21) Hornby, J. A., Luo, J. K., Stevens, J. M., Wallace, L. A., Kaplan, W., Armstrong, R. N., and Dirr, H. W. (2000) Equilibrium folding of dimeric class mu glutathione transferases involves a stable monomeric intermediate. *Biochemistry 39*, 12336−12344.

(22) Gildenhuys, S., Wallace, L. A., Burke, J. P., Balchin, D., Sayed, Y., and Dirr, H. W. (2010) Class Pi glutathione transferase unfolds via a dimeric and not monomeric intermediate: functional implications for an unstable monomer. *Biochemistry 49*, 5074−5081.

(23) Luo, J. K., Hornby, J. A., Wallace, L. A., Chen, J., Armstrong, R. N., and Dirr, H. W. (2002) Impact of domain interchange on conformational stability and equilibrium folding of chimeric class micro glutathione transferases. *Protein Sci. 11*, 2208−2217.

(24) Gildenhuys, S., Wallace, L. A., and Dirr, H. W. (2008) Stability and unfolding of reduced *Escherichia coli* glutaredoxin 2: a monomeric structural homologue of the glutathione transferase family. *Biochemistry 47*, 10801−10808.

(25) Vlamis-Gardikas, A., Åslund, F., Spyrou, G., Bergman, T., and Holmgren, A. (1997) Cloning, overexpression, and characterization of glutaredoxin 2, an atypical glutaredoxin from *Escherichia coli*. *J. Biol. Chem. 272*, 11236−11243.

(26) Beecham, J. M. (1992) Global analysis of biochemical and biophysical data. *Methods Enzymol. 210*, 37−54.

(27) Pace, C. N. (1986) Determination and analysis of urea and guanidine hydrochloride denaturation curves. *Methods Enzymol. 131*, 266−280.

(28) Zitzewitz, J. A., Bilsel, O., Luo, J., Jones, B. E., and Matthews, C. R. (1995) Probing the folding mechanism of a leucine zipper peptide by stopped flow circular dichroism spectroscopy. *Biochemistry 34*, 12812−12819.

(29) Bilsel, O., Zitzewitz, J. A., Bowers, K. E., and Matthews, C. R. (1999) Folding mechanism of the R-subunit of tryptophan synthase, an alpha/beta barrel protein: Global analysis highlights the interconversion of multiple native, intermediate and unfolded forms through parallel channels. *Biochemistry 38*, 1018−1029.

(30) McCoy, A. J., Grosse-Kunstleve, R. W., Adams, P. D., Winn, M. D., Sroroni, L. C., and Read, R. J. (2007) Phaser Crystallographic software. *J. Appl. Crystallogr. 40*, 658−674.

(31) Collaborative Computing Project No. 4. (1994) *Acta Crystallogr., Sect. D: Biol. Crystallogr. 50*, 760−763.

(32) Harrop., S. J., DeMaere, M. Z., Fairlie, W. D., Reztsova, T., Valenzuela, S. M., Mazzanti, M., Tonini, R., Qiu, M. R., Jankova, L., Warton, K., Bauskin, A. R., Wu, W. M., Pankhurst, S., Campbell, T. J., Breit, S. N., and Curmi, P. M. (2001) Crystal structure of a soluble form of the intracellular chloride ion channel CLIC1 (NCC27) at 1.4 Å resolution. *J. Biol. Chem. 276*, 44993−45000.

(33) Murshudov, G. N., Vagin, A. A., and Dodson, E. J. (1997) Refinement of macromolecular structures by the maximum-likelihood method. *Acta Crystallogr., Sect. D: Biol. Crystallogr. 53*, 240−255.

(34) Emsley, P., and Cowtan, K. (2004) Coot: model-building tools for molecular graphics. *Acta Crystallogr., Sect. D: Biol. Crystallogr. 60*, 2126−2132.

(35) Laskowski, R. A., Rullmannn, J. A., MacArthur, M. W., Kaptein, R., and Thornton, J. M. (1996) AQUA and PROCHECK-NMR: programs for checking the quality of protein structures solved by NMR. *J. Biomol. NMR 8*, 477−486.

(36) Davis, I. W., Leaver-Fay, A., Chen, V. B., Block, J. N., Kapral, G. J., Wang, X., Murray, L. W., Arendall, W. B., Snoeyink, J., Richardson, J. S., and Richardson, D. C. (2007) MolProbity: all-atom contacts and structure validation for proteins and nucleic acids. *Nucleic Acids Res. 35*, W375−383.

(37) Murzin, A. G., Brenner, S. E., Hubbard, T., and Chothia, C. (1995) SCOP: a structural classification of proteins database for the investigation of sequences and structures. *J. Mol. Biol. 247*, 536−540.

(38) Pettersen, E. F., Goddard, T. D., Huang, C. C., Couch, G. S., Greenblatt, D. M., Meng, E. C., and Ferrin, T. E. (2004) UCSF Chimera: A visualization system for exploratory research and analysis. *J. Comput. Chem. 25*, 1605−1612.

(39) Reynolds, C., Damerell, D., and Jones, S. (2009) ProtorP: a protein-protein interaction analysis server. *Bioinformatics 25*, 413−414.

(40) Jones, S., and Thornton, J. M. (1996) Principles of protein-protein interactions. *Proc. Natl. Acad. Sci. U. S. A. 93*, 13−20.

(41) Jones, S., Marin, A., and Thornton, J. M. (2000) Protein domain interfaces: .characterization and comparison with oligomeric protein interfaces. *Protein Eng. 13*, 77−82.

(42) Keskin, O., Ma, B., and Nussinov, R. (2005) Hot regions in protein--protein interactions: the organization and contribution of structurally conserved hot spot residues. *J. Mol. Biol. 345*, 1281−1294.

(43) Pace, C. N., and Scholtz, J. M. (1997) Measuring the conformational stability of a protein, in *Protein Structure: A Practical Approach* (Creighton, T. E., Ed.) 2nd ed., pp 299−321, IRL Press at Oxford University Press, Oxford.

(44) Soulages, J. L. (1998) Chemical Denaturation: Potential Impact of Undetected Intermediates in the Free Energy of Unfolding and *m*-Values Obtained from a Two-State Assumption. *Biophys. J. 75*, 484−492.

(45) Gulick, A. M., Goihl, A. L., and Fahl, W. E. (1992) Structural studies on human glutathione S-transferase pi. Family of native-specific monoclonal antibodies used to block catalysis. *J. Biol. Chem. 267*, 18946−18952.

(46) Martini, F., Aceto, A., Sacchetta, P., Bucciarelli, T., Dragani, B., and Di Ilio, C. (1993) Investigation of intra-domain and inter-domain interactions of glutathione transferase P1−1 by limited chymotryptic cleavage. *Eur. J. Biochem. 218*, 845−851.

(47) Aceto, A., Sacchetta, P., Bucciarelli, T., Dragani, B., Angelucci, S., Radatti, G. L., and Di Ilio, C. (1995) Structural and functional properties of the 34-kDa fragment produced by the N-terminal chymotryptic cleavage of glutathione transferase P1−1. *Arch. Biochem. Biophys. 316*, 873−878.

(48) Li, X., Keskin, O., Ma, B., Nussinov, R., and Liang, J. (2004) Protein-protein interactions: hot spots and structurally conserved residues often locate in complemented pockets that pre-organized in the unbound states: implications for docking. *J. Mol. Biol. 344*, 781−795.

(49) Xia, J. F., Zhao, X. M., Song, J., and Huang, D. S. (2010) APIS: accurate prediction of hot spots in protein interfaces by combining protrusion index with solvent accessibility. *BMC Bioinf. 11*, 174.

(50) Sayed, Y., Wallace, L. A., and Dirr, H. W. (2000) The hydrophobic lock-and-key intersubunit motif of glutathione transferase A1-A1: implications for catalysis, ligandin function and stability. *FEBS Lett. 465*, 169−172.

(51) Stenberg, G., Abdalla, A. M., and Mannervik, B. (2000) Tyrosine 50 at the subunit interface of dimeric human glutathione transferase P1-P1 is a structural key residue for modulating protein

stability and catalytic function. *Biochem. Biophys. Res. Commun. 271*, 59−63.

(52) Hornby, J. A., Codreanu, S. G., Armstrong, R. N., and Dirr, H. W. (2002) Molecular recognition at the dimer interface of a class Mu glutathione transferase: role of a hydrophobic interaction motif in dimer stability and protein function. *Biochemistry 41*, 14238−14247.

(53) Vargo, M. A., Nguyen, L., and Colman, R. F. (2004) Subunit interface residues of glutathione S-transferase A1-A1 that are important in the monomer−dimer equilibrium. *Biochemistry 43*, 3327−3335.

(54) Hegazy, U. M., Mannervik, B., and Stenberg, G. (2004) Functional role of the lock and key motif at the subunit interface of glutathione transferase P1-P1. *J. Biol. Chem. 279*, 9586−9596.

(55) Alves, C. S., Kuhnert, D. C., Sayed, Y., and Dirr, H. W. (2006) The intersubunit lock-and-key motif in human glutathione transferase A1−1: role of the key residues Met51 and Phe52 in function and dimer stability. *Biochem. J. 393*, 523−528.